CONTRAST MEDIA & MOLECULAR IMAGING

Received: 21 April 2015, Accepted: 8 June 2015, Published online in Wiley Online Library: 11 August 2015

(wileyonlinelibrary.com) DOI: 10.1002/cmmi.1656

Hyperpolarized ^{6}Li as a probe for hemoglobin oxygenation level

Riccardo Balzan[a†], Mor Mishkovsky[b,c*†], Yana Simonenko[d], Ruud B. van Heeswijk[c,f], Rolf Gruetter[b,c,e], Uzi Eliav[d], Gil Navon[d] and Arnaud Comment[a]

Hyperpolarization by dissolution dynamic nuclear polarization (DNP) is a versatile technique to dramatically enhance the nuclear magnetic resonance (NMR) signal intensity of insensitive long-T_1 nuclear spins such as ^{6}Li. The ^{6}Li longitudinal relaxation of lithium ions in aqueous solutions strongly depends on the concentration of paramagnetic species, even if they are present in minute amounts. We herein demonstrate that blood oxygenation can be readily detected by taking advantage of the ^{6}Li signal enhancement provided by dissolution DNP, together with the more than 10% decrease in ^{6}Li longitudinal relaxation as a consequence of the presence of paramagnetic deoxyhemoglobin. Copyright © 2015 John Wiley & Sons, Ltd.

Keywords: lithium; hyperpolarization; dynamic nuclear polarization; magnetic resonance; MRI; molecular imaging; blood; deoxyhemoglobin

1. INTRODUCTION

Oxygen delivery and consumption correlate with the physiological state of tissues and organs and affect their metabolism. Pathological situations are characterized by variations in oxygenation levels (1,2), which may directly affect treatment and recovery (3,4). Oxygen uptake can be measured by positron emission tomography (PET) imaging following the inhalation of $^{15}O_2$. However, the short ^{15}O half-life (2.1 min) limits its availability, as it requires an onsite cyclotron, and the use of ionizing radiation restricts the number of examinations per patient (5). Alternatively, the stable ^{17}O isotope can be used to probe oxygen metabolism by magnetic resonance (MR). Unlike ^{15}O PET, ^{17}O MR offers the advantage to selectively measure the metabolically generated $H_2^{17}O$ without confounding signals from the $^{17}O_2$ molecules bound to hemoglobin. However, the low gyromagnetic ratio of ^{17}O (5.77 MHz/T) and the short associated T_2* relaxation time (~2 ms) leads to low sensitivity (6). A different MR method for mapping oxygenation level is based on the blood oxygenation level dependent (BOLD) contrast, which relies on the effect of paramagnetic deoxyhemoglobin on proton transverse relaxation (7). Although BOLD MR imaging is mostly known in the context of cognitive neuroscience as functional MRI, recent studies have shown that it can be used to map hypoxic regions in tumors (8). The major drawback of this T_2*-weighted imaging approach lies in the dependence of T_2* on many parameters other than the oxygen level, including magnetic field inhomogeneities, water diffusion, and the structure of the blood vessel network including blood volume, which may represent confounding variables (9).

The recently developed dissolution dynamic nuclear polarization (DNP) technique enables hyperpolarizing nuclear spins of molecules in solutions that can be injected into cell suspensions, perfused organs, animals, or humans (10). The large signal resulting from the dramatic increase in polarization allows detection in real time of the biodistribution and the metabolism of molecules containing nuclear spins with long longitudinal relaxation times (11–13). Consequently, DNP-enhanced MR studies have been so far mostly restricted to precursors with non-protonated spin-½ nuclei such as ^{13}C-labeled carbonyls or ^{15}N-labeled quaternary amines. However, it has been shown that ^{6}Li, a spin-1 nucleus with an exceptionally small quadrupole moment ($Q < 8.5$ kHz), can also be hyperpolarized using dissolution DNP and that hyperpolarized ^{6}Li can be detected *in vivo* in the rat brain (14). The ^{6}Li longitudinal relaxation time of Li^+ ions can be as long as 550 s when dissolved in deoxygenated deuterated water (D_2O) at room temperature (15).

* *Correspondence to: M. Mishkovsky, Laboratory for Functional and Metabolic Imaging, Ecole Polytechnique Fédérale de Lausanne, CH-1015 Lausanne, Switzerland. E-mail: mor.mishkovsky@epfl.ch*

† *R.B. and M.M. contributed equally to this work.*

a *R. Balzan, A. Comment*
Institute of Physics of Biological Systems, Ecole Polytechnique Fédérale de Lausanne, CH-1015, Lausanne, Switzerland

b *M. Mishkovsky, R. Gruetter*
Laboratory for Functional and Metabolic Imaging, Ecole Polytechnique Fédérale de Lausanne, CH-1015, Lausanne, Switzerland

c *M. Mishkovsky, R. B. van Heeswijk, R. Gruetter*
Department of Radiology, Université de Lausanne, CH-1015, Lausanne, Switzerland

d *Y. Simonenko, U. Eliav, G. Navon*
School of Chemistry, Tel-Aviv University, Ramat-Aviv, Tel Aviv, Israel

e *R. Gruetter*
Department of Radiology, Geneva University Hospital and Faculty of Medicine, University of Geneva, CH-1211, Genève 4, Switzerland

f *R. B. van Heeswijk*
Center of Biomedical Imaging (CIBM), Lausanne, Switzerland

A recent study showed that, following the intraperitoneal administration of lithium to rodents, a large fraction of the Li^+ ions incorporated into the brain is located in the intracellular compartment (16). Hyperpolarized ^6Li could therefore be an interesting contrast medium for perfusion imaging with methods similar to those proposed with hyperpolarized xenon (17) and hyperpolarized ^{13}C tert-butanol (18). More generally, the potential of hyperpolarized ^6Li as contrast agent for molecular imaging is high because Li^+ ions can replace the ubiquitous and essential Na^+ ions in many biological systems. It was previously shown that the ^6Li T_1 of Li^+ ions in solutions is remarkably sensitive to the presence of paramagnetic species and that hyperpolarized ^6Li could be used as a sensor for trace amounts (<mM) of Gd-based MR contrast agents (14). The aim of the present study was to detect the blood oxygenation level in human and rat blood and plasma using hyperpolarized ^6Li.

2. RESULTS

To determine the effect of hemoglobin oxygenation on the T_1 of ^6Li, we simultaneously measured the decay of the hyperpolarized ^6Li signal in three separate tubes, two of them (Tubes 1 and 3) containing either whole blood and deoxygenated blood, or plasma and deoxygenated plasma, and the third one (Tube 2) containing D_2O (99.6% D) to obtain a reference relaxation measurement (Fig. 1). To separate the signals originating from each of the three tubes, one-dimensional projections (gradient echo) were acquired following non-selective 10° flip angle pulses applied every 20 s. Gradient strength was adjusted to maximize the signal per voxel while avoiding overlap between the signals originating from the three different tubes in the one-dimensional projection. In all measurements, the persistent radical which is necessary for the DNP process was scavenged with sodium ascorbate prior to the infusion of the hyperpolarized solution into the tubes (19). The ^6Li decay curves were obtained from each experiment by plotting the magnitude of the signal corresponding to each tube as a function of time (Fig. 2). The characteristic decay

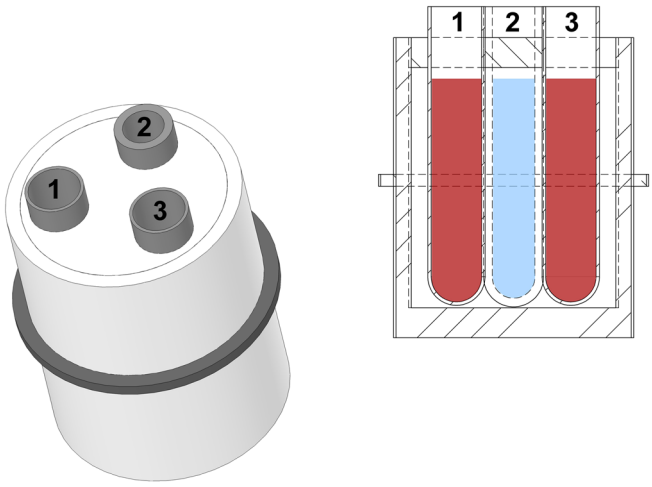

Figure 1. Left: schematic representation of the tube holder containing the three 10 mm glass tubes labeled from 1 to 3 and the surrounding 40 mm inner diameter coils. Tube 2 has thicker walls and served as a reference to assess the relaxation time of each hyperpolarized $^6Li^+$ solution. Tubes 1 and 3 served for the relative measurements between whole and deoxygenated blood or plasma. Right: cross section showing the arrangement of the three tubes inside the tube holder.

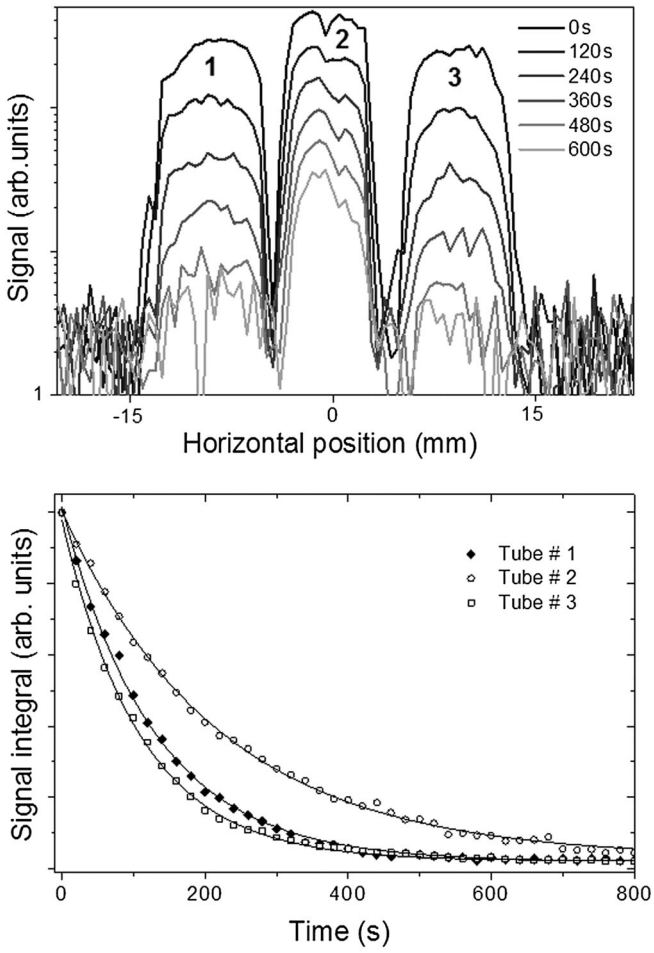

Figure 2. Top: time evolution of the tomographic projection of the ^6Li signal measured following the simultaneous injection of hyperpolarized $^6Li^+$ solution into all three tubes. Projections were acquired along the horizontal axis perpendicular to the static field using a 2.5 ms 6 G/cm dephasing gradient and a 20 ms 1.5 G/cm acquisition gradient. Bottom: integral of the projected ^6Li signal measured in Tubes 1–3 as a function of time.

constants were obtained by fitting the curves with mono-exponential functions. The longitudinal relaxation time T_1 was deduced after correcting for the effect of the pulses on the signal decay. The ^6Li T_1 values measured in blood and plasma samples are presented in Table 1.

To evaluate the effect of the radical scavenger on ^6Li T_1, measurements were made in thermally polarized 0.5 M ^6LiCl aqueous solutions (D_2O, 99.6% D) with or without scavenger (Table 2). The T_1 in pure non-deoxygenated D_2O (99.98 % D) was similar to the previously reported value for deoxygenated D_2O (15). Adding 20 mM of sodium ascorbate, in either its protonated or deuterated form, led to a decrease in T_1 of about 20%. Although the exchangeable protons of ascorbate increase the concentration of protonated water molecules and therefore participate in increasing the solvent-induced dipolar relaxation of ^6Li (20), the fact that the T_1 was nearly identical when ascorbate was deuterated shows that the most prominent relaxation mechanism induced by the presence of ascorbate is rather due to a direct interaction between Li^+ ions and ascorbate (a complete analysis of the relaxation mechanism is however beyond the scope of the present study). When performing hyperpolarized ^6Li MR experiments, it was observed that an ascorbate-to-radical ratio of 3 was

Table 1. Mean ^{6}Li longitudinal relaxation time measured in human and rat samples displayed with their standard deviation (SD) and relative standard deviation (RSD)

	^{6}Li T_1 (s)	SD (s)	RSD (%)
Human samples (130 mM ^{6}Li, n = 3)			
Whole blood	177	31	17.5
Deoxygenated blood	157	28	17.8
Plasma	115	7	6.1
Deoxygenated plasma	135	10	7.4
Rat samples (130 mM ^{6}Li, n = 3)			
Whole blood	180	19	10.5
Deoxygenated blood	153	12	7.8
Plasma	103	7	6.8
Deoxygenated plasma	123	5	4.0
Rat samples (0.65 mM ^{6}Li, n = 4)			
Whole blood	161	2	1.2
Deoxygenated blood	144	2	1.4
Plasma	137	4	2.9
Deoxygenated plasma	146	5	3.4

Table 2. Longitudinal relaxation time of ^{6}Li in various aqueous solutions. The measurements were made on a 400 MHz high-resolution MR system (Bruker BioSpin, Fällanden, Switzerland) using a saturation recovery protocol

Sample composition	^{6}Li T_1 (s)
0.5 M ^{6}LiCl in pure D_2O	506 ± 10
0.5 M ^{6}LiCl in D_2O with 20 mM deuterated sodium ascorbate	401 ± 5
0.5 M ^{6}LiCl in D_2O with 20 mM sodium ascorbate	394 ± 5
Hyperpolarized ^{6}LiCl solution (n = 6) (130 mM ^{6}Li in D_2O containing 1.2 mM ascorbate and 0.4 mM TEMPOL)	261 ± 5
Hyperpolarized ^{6}LiCl solution (n = 8) (0.65 mM ^{6}Li in deuterated phosphate buffer containing 0.45 mM ascorbate and 0.015 mM TEMPOL)	413 ± 15

insufficient to rapidly scavenge the 0.4 mM of nitroxyl radical present in the final solution, since a substantially shorter T_1 was recorded (Table 2). In a second series of experiments, performed with a drastically lower radical concentration corresponding to an ascorbate-to-radical ratio of 30 for an ascorbate concentration of 0.45 mM, the contribution of nitroxyl radicals to the ^{6}Li relaxation was effectively quenched and essentially negligible.

Two parameters were measured to assess the efficiency of the deoxygenation procedure: the partial pressure of oxygen (P_{O2}), representative of the concentration of free oxygen gas dissolved in the sample, as well as the oxygen saturation (S_{O2}), indicating the fraction of hemoglobin bound to oxygen. The relative decrease in P_{O2} following deoxygenation, namely $([P_{O2}]^{oxy} - [P_{O2}]^{deoxy})/[P_{O2}]^{oxy}$, was 5.2% in blood and 36% in plasma, and a relative reduction of $([S_{O2}]^{oxy} - [S_{O2}]^{deoxy})/[S_{O2}]^{oxy}$ = 2% was measured in blood (Table 3).

Table 3. Results of the oxygen gas analysis in blood and plasma samples. The measurements were made using a COBAS® b 121 system (Roche Diagnostic, Mannheim, Germany)

Samples (n = 3)	P_{O2} (mm Hg)	SD (mm Hg)	RSD (%)
Whole blood	45.9	0.6	1.3
Deoxygenated blood	43.5	0.5	1.1
Plasma	121.7	1.2	1.0
Deoxygenated plasma	77.9	13.4	17.2
	S_{O2} (%)	SD (%)	RSD (%)
Whole blood	76.9	0.3	0.4
Deoxygenated blood	75.4	0.7	0.9

The relative change in ^{6}Li longitudinal relaxation time following deoxygenation, namely $(T_1^{oxy} - T_1^{deoxy})/T_1^{oxy}$, was computed for each experiment (Fig. 3). We observed in all experiments that the ^{6}Li T_1 is shorter in deoxygenated blood than in whole blood, i.e. partially oxygenated blood, with a mean relative variation between 10 and 15%. Conversely, the observed ^{6}Li T_1 is longer in deoxygenated plasma than in partially oxygenated plasma. To confirm these results at pharmacologically relevant lithium level in anticipation of future *in vivo* studies, a series of experiment was carried out in rat blood and plasma using deuterated phosphate buffer instead of D_2O for dissolution. The same trend was observed with a relative change of +10.5% in rat blood and −6.5% in the plasma following deoxygenation. In this second series of experiments, the standard deviation on the relative differences was significantly lower (less than 10%).

3. DISCUSSION

The present study shows that hemoglobin oxygenation can be monitored through its influence on the hyperpolarized ^{6}Li longitudinal relaxation time. We chose to add ascorbate in the hyperpolarized ^{6}Li solutions not only to reduce the detrimental effect of the TEMPOL (4-hydroxy-2,2,6,6-tetramethylpiperidine-1-oxyl) radicals on the relaxation and therefore increase the T_1, but also to improve the reproducibility of the experiments since even slight changes in radical concentration can have a strong effect on the long ^{6}Li relaxation time. As was already observed

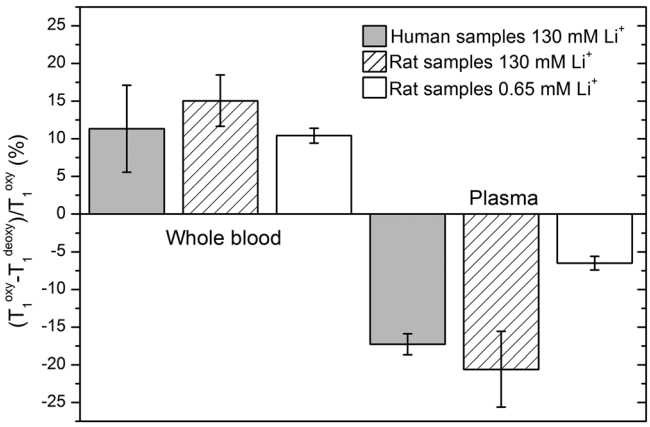

Figure 3. Mean relative change in ^{6}Li longitudinal relaxation time after deoxygenation of blood and plasma in both human and rat samples.

with hyperpolarized [1-^{13}C]acetate (20), a relatively large ascorbate-to-radical concentration ratio must be used to completely quench the radicals within the short hyperpolarized MR experiments. However, increasing the scavenger concentration above a certain threshold will also lead to increased relaxation induced by the presence of ascorbate molecules. A possible way to avoid this issue would be to use radicals such as BDPA (1,3-bisdiphenylene-2-phenylallyl), which can be easily filtered out since they precipitate in aqueous solutions (21).

Oxygenated hemoglobin being diamagnetic, it does not affect the ^{6}Li relaxation. By blowing argon gas on whole blood samples, oxyhemoglobin was transformed into deoxyhemoglobin. The shorter ^{6}Li T_1 observed in deoxygenated blood as compared with non-deoxygenated blood was ascribed to paramagnetic deoxyhemoglobin. The relative $(T_1^{oxy} - T_1^{deoxy})/T_1^{oxy}$ ratio in ^{6}Li longitudinal relaxation time is therefore positive in blood samples (Fig. 3). This effect is similar to the BOLD contrast which originates from the change in proton T_2* induced by the paramagnetic relaxation caused by the presence of deoxyhemoglobin. In contrast, in plasma, oxygen is present as molecular O_2, which is paramagnetic. Blowing argon removes O_2, thereby reducing the concentration of paramagnetic species from the plasma and leading to increased ^{6}Li T_1 values. The relative $(T_1^{oxy} - T_1^{deoxy})/T_1^{oxy}$ ratio is therefore negative in plasma (Fig. 3).

A non-negligible variability in the ^{6}Li T_1 values measured in blood and plasma samples was observed, in particular in experiments performed in the first series of experiments (Table 1). These variances were dramatically reduced in the second series of experiments performed with pharmacological doses of lithium, and substantially longer T_1 values were recorded in the plasma samples. These two observations led us to conclude once more that a large scavenger-to-radical ratio is necessary to limit the effect of the unavoidable slight variations in radical concentration on T_1 and, while in blood samples the contribution of deoxyhemoglobin to the ^{6}Li longitudinal relaxation is dominant, the nitroxyl radicals seem to be a non-negligible relaxation mechanism in plasma samples.

It also appears that the mean relative $(T_1^{oxy} - T_1^{deoxy})/T_1^{oxy}$ ratio measure in blood samples is rather similar in all experiments, ranging from 10.5 to 15%, whereas it varies from −6.5 to −20.5% in the plasma samples. This can be explained by the strikingly high variability in plasma P_{O2} following the deoxygenation procedure even within the same series of experiments (see Table 3). In addition, the blood and plasma samples used in the second series were more diluted than in the first series of experiments following the injection of 400 μL of hyperpolarized ^{6}Li in 1.5 mL of samples instead of 300 μL of hyperpolarized ^{6}Li in 2 mL samples (see the Experiment section). The oxygen concentration was therefore expected to be higher in the first series of experiments, meaning that a stronger effect of plasma deoxygenation could be expected.

When comparing the relative changes in T_1 measured in the second series of experiments with the results of the gas analyses, it appears that a 2% variation in blood oxygen level translates into a 10.5% change in ^{6}Li T_1, demonstrating the high sensitivity of the proposed method. Note that a relative variation of 36% in P_{O2} measured in plasma only corresponds to a 6.5% change in T_1, showing that the relaxation of ^{6}Li is remarkably more sensitive to the presence of deoxyhemoglobin than of molecular oxygen.

In a medical context, the primary use of lithium salts is to treat manic–depressive (bipolar) and depressive disorders (22,23). For ^{7}Li MR studies in humans (24), they have been administrated at doses up to 1200 mg/day, which led to serum concentration between 0.3 and 1 mM (25), a range similar to the concentration obtained after infusion of hyperpolarized [1-^{13}C]pyruvate in the first clinical study (26). We show that blood oxygenation can be monitored through its influence on the hyperpolarized ^{6}Li longitudinal relaxation time also when using pharmacological lithium doses. The observed difference in T_1 between whole and deoxygenated blood could therefore be possibly used to detect hemoglobin oxygenation level *in vivo*, and T_1-weighted ^{6}Li imaging could be considered to obtain oxygenation maps. This would be a particularly interesting diagnostic tool for assessing tumor oxygenation level, for instance prior to radiation therapy. It must, however, be borne in mind that the intracellular and extracellular ^{6}Li T_1 values might be substantially different and the interpretation of the results could be intricate.

4. EXPERIMENTAL

Fresh human venous blood samples were provided by healthy volunteers. Rat venous blood samples were collected by bleeding 10 male Sprague-Dawley rats (384 ± 40 g). Rats were anesthetized with 1.5% isoflurane in a 30% O_2/70% N_2O mixture. All animal experiments were performed according to federal and local ethical guidelines, and the protocols were approved by the local regulatory body (Service de la consommation et des affaires vétérinaires, Affaires vétérinaires, Canton de Vaud, Switzerland). 3 UI/mL of heparin (Drossapharm, Basel, Switzerland) was added to each human and animal blood sample. Samples were kept refrigerated at 5 °C in 50 mL Falcon tubes and were used within two days of blood withdrawal. Plasma was extracted from blood samples following natural phase separation in tubes stored in a vertical position at 5 °C.

MR measurements were carried out on an actively shielded horizontal 9.4 T/31 cm animal scanner (Varian/Magnex, Palo Alto, CA, USA) using a custom-designed ^{1}H/^{6}Li probe based on two stacked 40 mm inner diameter coils (machined from a double-sided printed circuit board) surrounding a cylindrical tube holder (Plexiglass) containing three 10 mm diameter glass tubes, two with thin 0.55 mm walls (513-1PS-7, Wilmad, Vineland, NJ, USA) and one with 1.45 mm wall thickness (513-7PPH-7, Wilmad, Vineland, NJ, USA). The geometry of the tube holder was designed so that the horizontal tomographic projection of each of the three tubes is well separated from one another (Fig. 1). In all experiments the tube holder was inserted inside the magnet bore prior to each dissolution DNP experiment. Proton images were acquired to position the tube holder at the magnet isocenter and static field inhomogeneities were corrected by manual shimming. The deoxygenation process consisted in blowing argon gas inside the glass tube containing either blood or plasma for 10 min, about 5 min prior to the dissolution experiment. Heavy noble gas was preferred over nitrogen gas to prevent air from reoxygenating the samples before and during MR acquisitions. Each tube was then covered with a perforated plastic cap. A polytetrafluoroethylene (PTFE) capillary was inserted through the cap to remotely inject the hyperpolarized $^6Li^+$ solution into the sample.

A first series of experiments was performed in both human and rat blood using a $^6Li^+$ concentration of 130 mM. A set of three 2 mL samples each inserted in one glass tube was probed:

Tube 1 and Tube 3 contained either whole blood and deoxygenated blood or plasma and deoxygenated plasma. Tube 2 was filled with pure D_2O and served as a reference to assess the relaxation time of each hyperpolarized $^{6}Li^{+}$ solution. Prior to each experiment, 350 μL of 15 M ^{6}LiCl solution prepared in 2:1 D_2O/d_6-ethanol (v/v) doped with 40 mM TEMPOL was inserted, in the form of 2 mm diameter frozen beads, inside a custom-designed 7 T polarizer (27). 50 μL of frozen 1 M aqueous sodium ascorbate solution was added inside the sample cup to scavenge the TEMPOL radicals during the dissolution process (19). All chemicals were purchased from Sigma-Aldrich (Buchs, Switzerland). After 1 h of polarization at 1 ± 0.05 K, the samples were rapidly dissolved in 5 mL of superheated D_2O (180 °C) and the resulting hyperpolarized $^{6}Li^{+}$ solution was collected out of the polarizer by blowing high-pressure helium gas (6 bar) for 3.5 s through the dissolution insert previously described (28). 300 μL of solution was manually and sequentially injected into each 10 mm tube through a PTFE capillary within 10 s. Data acquisition started 20 s after dissolution. The liquid-state ^{6}Li polarization at the time of measurements was estimated to be 5 ± 0.3% from a comparison between the hyperpolarized and the thermally polarized ^{6}Li signals.

To confirm these observations at pharmacologically relevant Li^{+} level, a second series of experiments was performed in rat blood and plasma. For these experiments, Tube 1 and Tube 3 were filled with 1.5 mL of either whole blood and deoxygenated blood or plasma and deoxygenated plasma. Tube 2 was filled with 1.5 mL of pure D_2O. An amount of 5 μL of 3 M ^{6}LiCl frozen solution prepared in 1:1 D_2O/glycerol-d_8 (w/w) doped with 58 mM TEMPOL was inserted inside the polarizer along with 10 μL of frozen 1 M aqueous sodium ascorbate solution. The concentration of lithium salt was reduced from 15 M to 3 M to avoid inaccuracy in sample volume when preparing the frozen beads. Polarization time was set to 1.5 h and the samples were dissolved in 5 mL of superheated deuterated phosphate buffer. The liquid-state ^{6}Li polarization was 7.4 ± 0.5%. After having collected the hyperpolarized $^{6}Li^{+}$ solution, 400 μL of solution was manually and sequentially injected prior to data acquisition. The other parameters were identical to the ones set in the first series of experiments.

In conjunction with the hyperpolarized ^{6}Li MR experiments, oxygen gas analysis was performed in samples prepared in the exact same way than those used in the second series of experiments. For these analyses, 100 μL aliquots of blood or plasma were taken from each sample and the P_{O2} and S_{O2} values were obtained using a COBAS® b 121 system (Roche Diagnostic, Mannheim, Germany).

Acknowledgments

We thank Dr Mario Lepore for his help with animal handling and blood analyses. The authors declare no competing financial interests. This work was supported by the Swiss National Science Foundation (grant 200020_124901 and PP00P2_133562 to A.C. and grant 31003A_131087 to R.G.), the Centre d'Imagerie BioMédicale (CIBM) of the UNIL, UNIGE, HUG, CHUV, EPFL, and the Leenards and Jeantet Foundations.

REFERENCES

1. Ishii K, Kitagaki H, Kono M, Mori E. Decreased medial temporal oxygen metabolism in Alzheimer's disease shown by PET. J Nucl Med 1996; 37(7): 1159–1165.
2. Karimi M, Golchin N, Tabbal SD, Hershey T, Videen TO, Wu J, Usche JWM, Revilla FJ, Hartlein JM, Wernle AR, Mink JW, Perlmutter JS. Subthalamic nucleus stimulation-induced regional blood flow responses correlate with improvement of motor signs in Parkinson disease. Brain 2008; 131: 2710–2719.
3. Brown JM, William WR. Exploiting tumour hypoxia in cancer treatment. Nat Rev Cancer 2004; 4(6): 437–447.
4. Rother J, Schellinger PD, Gass A, Siebler M, Villringer A, Fiebach JB, Fiehler J, Jansen O, Kucinski T, Schoder V, Szabo K, Junge-Hulsing GJ, Hennerici M, Zeumer H, Sartor K, Weiller C, Hacke W, Stu KS. Effect of intravenous thrombolysis on MRI parameters and functional outcome in acute stroke < 6 hours. Stroke 2002; 33(10): 2438–2445.
5. Baron JC, Jones T. Oxygen metabolism, oxygen extraction and positron emission tomography: Historical perspective and impact on basic and clinical neuroscience. Neuroimage 2012; 61(2): 492–504.
6. Gordji-Nejad A, Mollenhoff K, Oros-Peusquens AM, Pillai DR, Shah NJ. Characterizing cerebral oxygen metabolism employing oxygen-17 MRI/MRS at high fields. Magn Reson Mater Phys Biol Med 2014; 27(1): 81–93.
7. Ogawa S, Lee TM, Kay AR, Tank DW. Brain magnetic-resonance-imaging with contrast dependent on blood oxygenation. Proc Natl Acad Sci U S A 1990; 87(24): 9868–9872.
8. Price JM, Robinson SP, Koh DM. Imaging hypoxia in tumours with advanced MRI. Q J Nucl Med Mol Imaging 2013; 57(3): 257–270.
9. Christen T, Lemasson B, Pannetier N, Farion R, Remy C, Zaharchuk G, Barbier EL. Is T2* enough to assess oxygenation? Quantitative blood oxygen level-dependent analysis in brain tumor. Radiology 2012; 262(2): 495–502.
10. Ardenkjaer-Larsen JH, Fridlund B, Gram A, Hansson G, Hansson L, Lerche MH, Servin R, Thaning M, Golman K. Increase in signal-to-noise ratio of > 10,000 times in liquid-state NMR. Proc Natl Acad Sci U S A 2003; 100(18): 10158–10163.
11. Gallagher FA, Kettunen MI, Brindle KM. Biomedical applications of hyperpolarized C-13 magnetic resonance imaging. Prog Nucl Magn Reson Spectrosc 2009; 55(4): 285–295.
12. Golman K, in't Zandt R, Thaning M. Real-time metabolic imaging. Proc Natl Acad Sci U S A 2006; 103(30): 11270–11275.
13. Kurhanewicz J, Vigneron DB, Brindle K, Chekmenev EY, Comment A, Cunningham CH, DeBerardinis RJ, Green GG, Leach MO, Rajan SS, Rizi RR, Ross BD, Warren WS, Malloy CR. Analysis of cancer metabolism by imaging hyperpolarized nuclei: prospects for translation to clinical research. Neoplasia 2011; 13(2): 81–97.
14. van Heeswijk RB, Uffmann K, Comment A, Kurdzesau F, Perazzolo C, Cudalbu C, Jannin S, Konter JA, Hautle P, van den Brandt B, Navon G, van der Klink JJ, Gruetter R. Hyperpolarized lithium-6 as a sensor of nanomolar contrast agents. Magn Reson Med 2009; 61(6): 1489–1493.
15. Wehrli FW. Temperature-dependent spin–lattice relaxation of Li-6 in aqueous lithium-chloride. J Magn Reson 1976; 23(3): 527–532.
16. Komoroski RA, Lindquist DM, Pearce JM. Lithium compartmentation in brain by ^{7}Li MRS: effect of total lithium concentration. NMR Biomed 2013; 26(9): 1152–1157.
17. Sun Y, Schmidt NO, Schmidt K, Doshi S, Rubin JB, Mulkern RV, Carroll R, Ziu M, Erkmen K, Poussaint TY, Black P, Albert M, Burstein D, Kieran MW. Perfusion MRI of U87 brain tumors in a mouse model. Magn Reson Med 2004; 51(5): 893–899.
18. Grant AK, Vinogradov E, Wang XE, Lenkinski RE, Alsop DC. Perfusion imaging with a freely diffusible hyperpolarized contrast agent. Magn Reson Med 2011; 66(3): 746–755.
19. Mieville P, Ahuja P, Sarkar R, Jannin S, Vasos PR, Gerber-Lemaire S, Mishkovsky M, Comment A, Gruetter R, Ouari O, Tordo P, Bodenhausen G. Scavenging free radicals to preserve enhancement and extend relaxation times in NMR using dynamic nuclear polarization. Angew Chem Int Ed 2010; 49(35): 6182–6185.
20. Cheng T, Mishkovsky M, Bastiaansen JAM, Ouari O, Hautle P, Tordo P, van den Brandt B, Comment A. Automated transfer and injection of hyperpolarized molecules with polarization measurement prior to *in vivo* NMR. NMR Biomed 2013; 26(11): 1582–1588.
21. Lumata L, Ratnakar SJ, Jindal A, Merritt M, Comment A, Malloy C, Sherry AD, Kovacs Z. BDPA: an efficient polarizing agent for fast dissolution dynamic nuclear polarization NMR spectroscopy. Chemistry 2011; 17(39): 10825–10827.
22. Cade JF. Lithium salts in the treatment of psychotic excitement. Med J Aust 1949; 2(10): 349–352.

23. Thase ME, Denko T. Pharmacotherapy of mood disorders. Annu Rev Clin Psychol 2008; 4: 53–91.
24. Kushnir T, Itzchak Y, Valevski A, Lask M, Modai I, Navon G. Relaxation times and concentrations of 7Li in the brain of patients receiving lithium therapy. NMR Biomed 1993; 6(1): 39–42.
25. Lee JH, Adler C, Norris M, Chu WJ, Fugate EM, Strakowski SM, Komoroski RA. 4-T ^{7}Li 3D MR spectroscopy imaging in the brains of bipolar disorder subjects. Magn Reson Med 2012; 68(2): 363–368.
26. Nelson SJ, Kurhanewicz J, Vigneron DB, Larson PE, Harzstark AL, Ferrone M, van Criekinge M, Chang JW, Bok R, Park I, Reed G, Carvajal L, Small EJ, Munster P, Weinberg VK, Ardenkjaer-Larsen JH, Chen AP, Hurd RE, Odegardstuen LI, Robb FJ, Tropp J, Murray JA. Metabolic imaging of patients with prostate cancer using hyperpolarized [1-^{13}C]pyruvate. Sci Transl Med 2013; 5(198): 198ra108.
27. Cheng T, Capozzi A, Takado Y, Balzan R, Comment A. Over 35% liquid-state C-13 polarization obtained via dissolution dynamic nuclear polarization at 7 T and 1 K using ubiquitous nitroxyl radicals. Phys Chem Chem Phys 2013; 15(48): 20819–20822.
28. Comment A, van den Brandt B, Uffmann K, Kurdzesau F, Jannin S, Konter JA, Hautle P, Wenckebach WT, Gruetter R, van der Klink JJ. Design and performance of a DNP prepolarizer coupled to a rodent MRI scanner. Concepts Magn Reson B 2007; 31B(4): 255–269.